On evaluating the reaction path Hamiltonian

Michael Page and James W. McIver

Additional information on J. Chem. Phys.

On evaluating the reaction path Hamiltonian

Michael Page
Laboratory for Computational Physics and Fluid Dynamics, Naval Research Laboratory, Washington, D. C. 20375

James W. McIver, Jr.
Department of Chemistry, State University of New York at Buffalo, Buffalo, New York 14214

This paper examines a number of aspects of evaluating the reaction path Hamiltonian (RPH) of Miller, Handy, and Adams. The reaction path is represented as a Taylor series expansion of mass weighted Cartesian coordinates as a function of arc length. The second (path tangent) and third (path curvature) coefficients in the Taylor series are important in the RPH. General analytical formulas for all the coefficients as explicit functions of energy derivatives are derived. If the Taylor series is expanded about the saddle point, special limiting formulas for the coefficients are required. These are obtained using L'Hospital's rule. In a local quadratic approximation (LQA) third and higher energy derivatives are ignored. Within this approximation all but the first two coefficients in the Taylor series expansion of the path are zero when the expansion point is the saddle point. At nonstationary points on the path the first three Taylor series coefficients are evaluated exactly within the LQA while the others have nonzero approximate values. The resulting LQA Taylor series can be summed exactly. This leads to a new method of stepping along the reaction path which is superior to the traditional Euler method and should be used whenever second energy derivatives are available. Extensions of this method which include third energy derivative information are also presented. Exact analytical formulas for the RPH coupling parameters are derived. These include simplified formulas for the projection matrix and its derivative. At nonstationary points, the couplings of the transverse vibrations to the path depend only on first and second energy derivatives and hence are exactly calculated in the LQA. The remaining RPH parameters depend on third energy derivatives as well but have nonzero approximate values in the LQA. At the saddle point, all of the RPH parameters depend on third energy derivatives and they are zero when third derivatives are ignored. In general, when the complete set of RPH parameters are calculated, the same energy derivative information is required at the saddle point as at nonstationary points, namely the gradient, the force constants, and the components of the third derivatives along the path tangent. It is demonstrated that severe errors can occur when the RPH parameters are calculated at a point near the saddle point lying on the eigenvector corresponding to the negative eigenvalue of the force constant matrix at the saddle point. These errors occur even when the exact formulas are used and are due to slight deviations of this eigenvector from the exact reaction path. A remedy is described.

I. INTRODUCTION

Perhaps the most significant recent advance in the dynamical study of polyatomic systems is the reaction path Hamiltonian (RPH) introduced by Miller, Handy, and Adams.[1] This Hamiltonian is particularly well suited for use with potential energies obtained from *ab initio* calculations because of its focus on a very small region of configuration space. The growing number of dynamical studies of polyatomic systems based on the RPH have recently been reviewed by Miller[2] and by Truhlar and co-workers.[3–5] Our own interest has been in the study of radicals, radical pairs, and biradicals[6] using canonical variational transition state theory.[7]

There are a number of interesting and important computational aspects of evaluating the RPH. When used with *ab initio* methods, one seeks a sufficiently accurate RPH at a minimum cost. The central problem has been locating the reaction path and making suitable corrections when one has strayed from it. This has received considerable attention in the literature.[8,9] Other problems occur when attempting to evaluate RPH parameters near the saddle point where the normalized energy gradient becomes indeterminate.

The purpose of this paper is to derive and analyze formulas for determining the reaction path and evaluating the RPH coupling parameters. These formulas differ from those previously used in that they *explicitly* involve the derivatives of the potential energy with respect to mass weighted Cartesian coordinates and they can also be used at the saddle point.

Besides any asthetic value there are a number of important interpretational and computational advantages such exact analytical formulas have over finite difference or other approximate techniques. Numerical accuracy problems due to differencing are avoided and other instabilities can be isolated by making explicit the implicit dependence on geometry and energy derivatives. By showing exactly how third and higher energy derivatives with respect to (mass weighted) Cartesian coordinates enter, we can separately measure

their contributions to the RPH coupling parameters. A special case of this is neglecting or otherwise approximating third and higher energy derivatives. In this paper, e.g., we show that only the first and second energy derivatives are required to exactly compute the path curvature at nonstationary points, and that inclusion of only the components of the third derivatives along the reaction path allows all of the RPH parameters to be computed exactly. Finally, Cartesian energy derivatives can be efficiently and accurately evaluated analytically for an increasingly broad class of *ab initio* methods.[10]

We are also able to interpret the results of a calculation using analytical formulas in terms of well defined concepts. We can separately identify contributions to the RPH parameters due to projecting out translations, rotations, and the path tangent, for example.

The bulk of this paper is divided into two major sections. The first addresses the problem of defining the reaction path and evaluating its properties. In it we represent the path as a Taylor series expansion in the arc length about an arbitrary point on the path. We give general formulas for the expansion coefficients in terms of the energy derivatives. The special limiting forms of the formulas valid at the saddle point are discussed. In this section we also present and discuss a new method for following the reaction path that should be used when second energy derivatives are calculated. Finally we examine, explain, and solve the problem of numerical instabilities that occur when attempting to compute the path curvature near the saddle point.

In the second major section we derive and discuss the analytical formulas for the coupling elements in the RPH. At nonstationary points, the resulting formulas for all the RPH coupling parameters are represented by the sum of two terms, one of which depends only on first and second energy derivatives and the other on some third derivatives as well (the components along the path tangent). The formula for the important couplings of the transverse vibrations to the reaction path are shown to depend only on second energy derivatives. At the saddle point the formulas give zero for all the RPH coupling parameters if the third derivatives are ignored. Given the required energy derivatives the formulas require negligible amounts of additional computer time.

The last section briefly summarizes the results and offers some concluding remarks.

Four appendices contain details of the derivations of the Taylor series coefficients (Appendices A and B), the path curvature near the saddle point (Apppendix C), and new analytical formulas for the projection matrix and its derivative with respect to arc length (Appendix D).

II. THE REACTION PATH

A. Definition and properties

The first task in finding the reaction path is the location of the saddle point or transition structure for the reaction. The extensive literature on this subject has been most recently reviewed by Schlegel.[8(d)] We assume this structure is known. We do not consider here reactions for which there is no saddle point.

The reaction path is a line in mass weighted configuration space given parametrically in terms of its arc length s. We represent this line by $\mathbf{x}(s)$ where $\mathbf{x}$ is a column vector whose components are the $3N$ mass weighted Cartesian coordinates. The arc length s is defined by

$$ds^2 = \sum_{i=1}^{3N} dx_i^2. \tag{1}$$

The definition is completed by stating that $\mathbf{x}(s)$ is the solution to the set of autonomous first order ordinary differential equations:

$$\mathbf{v}(s) \equiv \mathbf{v}^{(0)}(s) \equiv \frac{d\mathbf{x}(s)}{ds} = \mathbf{g}/c \tag{2}$$

that approaches the saddle point from below.[9] The column vector $\mathbf{g}$ is the energy gradient in mass weighted Cartesian coordinates

$$g_i = \frac{\partial E}{\partial x_i}, \tag{3}$$

and the normalization constant is

$$c = \sqrt{\mathbf{g}^\dagger \mathbf{g}}. \tag{4}$$

The superscript (0) in Eq. (2) indicates the zero[th] derivative of the normalized path tangent $\mathbf{v}$ with respect to s. The superscript (n) will mean the nth derivative. We will use no superscript and (0) interchangeably.

In Eq. (2), we have arbitrarily chosen the tangent vector $\mathbf{v}$ to lie along the steepest ascent as opposed to steepest descent direction. It is convenient to regard the reaction path as having two branches, a "reactant" branch and "product" branch, which join smoothly at the saddle point. The path is then steepest ascent for the reactant branch and steepest descent for the product branch. For the product branch, $\mathbf{g}$ in Eq. (2) is replaced by its negative.

We have omitted the requirement that at the saddle point, $\mathbf{v}$ lies along the eigenvector of the force constant matrix corresponding to the negative eigenvalue. This result is a consequence of the definition.[11]

A dynamically important property of the reaction path is the curvature vector which is defined as

$$\mathbf{v}^{(1)} \equiv \frac{d\mathbf{v}}{ds} = \frac{d^2\mathbf{x}}{ds^2}. \tag{5}$$

Unlike Eq. (2), Eq. (5) is the same whether the path is defined as steepest ascent or steepest descent. The curvature vector is orthogonal to the tangent $\mathbf{v}$ but it is not normalized. Instead, the scalar curvature is defined as

$$\kappa(s) = \sqrt{\mathbf{v}^{(1)\dagger} \mathbf{v}^{(1)}}. \tag{6}$$

The curvature vector can be evaluated by differentiating Eq. (2) with respect to s. The result is

$$\mathbf{v}^{(1)} = [\mathbf{F}\mathbf{v} - (\mathbf{v}^\dagger \mathbf{F}\mathbf{v})\mathbf{v}]/c, \tag{7}$$

where $\mathbf{F}$ is the mass weighted force constant martrix

$$F_{ij} = \frac{\partial^2 E}{\partial x_i \partial x_j} = \frac{\partial g_i}{\partial x_j} = \frac{\partial g_j}{\partial x_i}. \tag{8}$$

In obtaining Eq. (7) we first note that the gradient depends on s only implicitly through its dependence on $\mathbf{x}$ so that chain rule differentiation of $\mathbf{g}$ gives

$$\frac{d\mathbf{g}}{ds} = \mathbf{F}\mathbf{v}, \tag{9}$$

where Eqs. (2) and (8) have been used. Equation (7) is obtained by differentiating Eq. (2) with respect to s and using Eq. (9) in the result.

Higher derivatives of the reaction path with respect to s can be obtained in a similar manner. The general formula for $\mathbf{v}^{(n)}$ is

$$\mathbf{v}^{(n)} = c^{-1} \sum_{k=0}^{n-1} \left[\binom{n-1}{k} \mathbf{F}^{(n-1-k)} - \binom{n}{k} c^{(n-k)} \mathbf{I} \right] \mathbf{v}^{(k)}, \tag{10}$$

where

$$c^{(i+1)} = \sum_{l=0}^{i} \sum_{m=0}^{l} \binom{i}{l}\binom{l}{m} \mathbf{v}^{(i-l)\dagger} \mathbf{F}^{(l-m)} \mathbf{v}^{(m)}. \tag{11}$$

The $\mathbf{F}^{(n)}$ are given by

$$F_{ij}^{(1)} = \sum_{k} G_{ijk} v_k = \sum_{k} \frac{\partial^3 E}{\partial x_i \partial x_j \partial x_k} v_k,$$

$$F_{ij}^{(2)} = \sum_{k} G_{ijk} v_k^{(1)} + \sum_{k}\sum_{l} H_{ijkl} v_k^{(0)} v_l^{(0)}, \tag{12}$$

$$F_{ij}^{(3)} = \sum_{k} G_{ijk} v_k^{(2)} + 3 \sum_{k}\sum_{l} H_{ijkl} v_k^{(0)} v_l^{(1)}$$

$$+ \sum_{k}\sum_{l}\sum_{m} J_{ijklm} v_k^{(0)} v_l^{(0)} v_m^{(0)}, \text{ etc.,}$$

where G_{ijk}, H_{ijkl}, and J_{ijklm} are third, fourth, and fifth energy derivatives, respectively. The symbol $\binom{n}{k}$ is the usual binomial coefficient. The summations are over the $3N$ mass weighted Cartesian coordinates. The derivation of Eq. (10) is not difficult and is given in Appendix A.

Equations (2), (7), and (10) ultimately depend only upon the energy derivatives evaluated at any given point in configuration space (excluding for the moment stationary points). Given any point on the path $\mathbf{x}_0 = \mathbf{x}(s_0)$, the path itself can be represented as a Taylor series in s expanded about $\mathbf{x}_0$,

$$\mathbf{x}(s) = \mathbf{x}(s_0) + \mathbf{v}^{(0)}(s - s_0) + \tfrac{1}{2}\mathbf{v}^{(1)}(s - s_0)^2 + \cdots$$

$$+ \frac{1}{n!} \mathbf{v}^{(n-1)}(s - s_0)^n + \cdots, \tag{13}$$

where the coefficients $\mathbf{v}^{(n)}$ depend only on energy derivatives evaluated at $\mathbf{x}_0$. Note that $\mathbf{v}^{(n-1)}$ in Eq. (13) is the nth derivative of the path. This specification of a unique path is a consequence of the existence and uniqueness theorems statisfied by the autonomous system [Eq. (2)]. Any point in configuration space lies on one and only one solution to Eq. (2).

This Taylor Series representation of the path forms the basis of a number of numerical integration methods. The simple and commonly used Euler method, e.g., uses only the first two terms of Eq. (13). In a many-dimensional problem a single Euler step gives at best only a component of the path lying on a line. Similarly, inclusion of the first three terms of Eq. (13) can give no more than the projection of the path onto the plane formed by the vectors $\mathbf{v}_0$ and $\mathbf{v}_0^{(1)}$. A three-dimensional path such as a corkscrew requires at least three

independent vectors. In general, a minimum of $3N$ independent vectors [e.g., either $3N + 1$ terms of Eq. (13) or $3N$ Euler steps] are required to describe the path in its full dimensionality.

Equation (13) refers to a Taylor series expansion of the Cartesian coordinate representation of the reaction path in terms of the arc length parameter s. There is another relevant Taylor series expansion: that of the potential energy in terms of the atomic Cartesian displacements. We will refer to the expansion of the energy truncated to second order as the local quadratic approximation (LQA) and this expansion truncated to third order as the local cubic approximation (LCA). These references to truncating the energy expansion should not be confused with truncating the Taylor series expansion of the path. In fact, for the path expansion within the LQA $\mathbf{v}$ and $\mathbf{v}^{(1)}$ will be computed exactly and all higher derivatives of $\mathbf{v}$ with respect to s will have nonzero approximate values. One can include, within the LQA, as many vectors in Eq. (13) as one wishes to compute by inserting the values of the computed gradient and force constant matrix into the formulas for the path derivatives. This, however, turns out not to be necessary in the LQA. If we adopt an alternative parametrization of the path, introduced by Pechukas,[11] then the corresponding infinite LQA Taylor series can be summed exactly. The resulting LQA formula for the reaction path should offer an improvement over the Euler method (which results from a local linear approximation to the energy) since a single step along this LQA path will include the correct path curvature at the point of expansion and in addition will include the full dimensionality. This method is discussed in Sec. II C.

The formulas for the path derivatives, Eqs. (7) and (10), are exact. As we will show later, however, severe numerical difficulties emerge when one attempts to use them near the saddle point. These difficulties are not due to the expected roundoff errors resulting from the small denominators of these equations, but are of a more profound nature. They are due to the fact that the reaction path itself is imprecisely determined. As the saddle point is approached, solutions to Eq. (2) that are initially close to the reaction path will veer off sharply. The $\mathbf{v}^{(1)}$ and higher derivatives of these paths will differ markedly from the correct values as a result. Nevertheless, the formulas for the reaction path derivatives at the saddle point can be obtained by a suitable limiting procedure. This is described in Sec. II B.

B. Behavior at the saddle point

It is obvious that Eq. (2) becomes indeterminate at the saddle point. Its limiting value can be obtained from L'Hospital's rule. This value can then be used to show that Eq. (7) also becomes indeterminate (rather than infinite) at the saddle point, and its limiting value can thus be obtained by L'Hospital's rule. By continuing this process we can obtain formulas for all of the reaction path derivative vectors at the saddle point. In general, these vectors depend upon the direction of approach to the saddle point, the correct values being obtained by approaching it along the reaction path.

This general derivation is outlined in Appendix B. The limiting formulas depend only upon the energy derivatives

evaluated at the saddle point and will be the same regardless of whether the saddle point is approached from the reactant or product side so long as it is approached along the reaction path. A Taylor series expansion of the reaction path about the saddle point will thus encompass both the reactant and product branches.

From Appendix B, the path tangent $\mathbf{v}^{(0)}(= \mathbf{v})$ at the saddle point is uniquely obtained as the eigenvector of the force constant matrix corresponding to the single negative eigenvalue

$$\mathbf{F}\mathbf{v} - (\mathbf{v}^\dagger \mathbf{F}\mathbf{v})\mathbf{v} = 0. \tag{14}$$

This result is equivalent to Pechukas'[11] but is obtained in a rather different manner. The general formula for higher path derivatives $\mathbf{v}^{(n)}$ at the saddle point is obtained as the solution to the linear system

$$\mathbf{M}(n)\mathbf{v}^{(n)} = \mathbf{T}_n, \quad n > 0, \tag{15}$$

where the symmetric matrix $\mathbf{M}(n)$ is given by

$$\mathbf{M}(n) = (n+1)\mathbf{v}^\dagger \mathbf{F}\mathbf{v}\mathbf{I} + 2\mathbf{v}\mathbf{v}^\dagger \mathbf{F} - \mathbf{F}, \quad n > 0. \tag{16}$$

The second term is symmetric because $\mathbf{v}$ is an eigenvector of $\mathbf{F}$, Eq. (14). The vectors $\mathbf{T}_n$ are

$$\mathbf{T}_1 = \mathbf{F}^{(1)}\mathbf{v} - \mathbf{v}^\dagger \mathbf{F}^{(1)}\mathbf{v}\mathbf{v}, \tag{17}$$

$$\begin{aligned}
\mathbf{T}_n = &\sum_{k=1}^n \binom{n}{k}\mathbf{F}^{(k)}\mathbf{v}^{(n-k)} - \sum_{k=2}^n \binom{n+1}{k}c^{(k)}\mathbf{v}^{(n+1-k)} \\
&- \sum_{k=1}^n \binom{n}{k}\mathbf{v}^{(n-k)\dagger}\mathbf{F}^{(k)}\mathbf{v}\mathbf{v} \\
&- \sum_{k=1}^{n-1}\sum_{l=0}^k \binom{n}{k}\binom{k}{l}\mathbf{v}^{(l)\dagger}\mathbf{F}^{(k-l)}\mathbf{v}^{(n-k)}\mathbf{v}, \quad n > 1,
\end{aligned} \tag{18}$$

where the $\mathbf{F}^{(i)}$ and $c^{(i)}$ are given by Eqs. (8), (12), and (11).

The matrix $\mathbf{M}(n)$ [Eq. (18)] is negative definite as is easily seen by evaluating it in a normal coordinate system, in which $\mathbf{F}$ is diagonal. Therefore, there are no problems with solving the linear system [Eq. (15)] and the solution is unique.

Every term in $\mathbf{T}_n$ is proportional to third or higher energy derivatives.[12] Therefore, in the LQA only the path tangent $\mathbf{v}$ [Eq. (14)] is nonzero at the saddle point. In particular, the curvature vector $\mathbf{v}^{(1)}$ at the saddle point, which can be written as

$$\mathbf{v}^{(1)} = (2\mathbf{v}^\dagger \mathbf{F}\mathbf{v}\mathbf{I} - \mathbf{F})^{-1}(\mathbf{F}^{(1)}\mathbf{v} - \mathbf{v}^\dagger \mathbf{F}^{(1)}\mathbf{v}\mathbf{v}), \tag{19}$$

would incorrectly by predicted to be zero in the LQA. In obtaining Eq. (19) the second term in $\mathbf{M}(1)$ [Eq. (16)] does not contribute because of the orthogonality of $\mathbf{v}$ and $\mathbf{v}^{(1)}$.

Evaluating the path curvature at the saddle point thus requires the components of the third derivatives along the path tangent $\mathbf{F}^{(1)}$. These can be found by a simple finite difference procedure such as

$$\mathbf{F}^{(1)} = \frac{d\mathbf{F}}{ds} \approx [\mathbf{F}(s_0 + \delta s) - \mathbf{F}(s_0 - \delta s)]/(2\delta s). \tag{20}$$

On the other hand, if all of the third derivatives are available (as might be the case when including anharmonic correc-

tions) then $\mathbf{v}^{(1)}$ can be evaluated analytically using Eq. (12). The calculation of two extra force constant matrices to obtain $\mathbf{F}^{(1)}$ at the saddle point is advisable for two reasons. First, as shown in Sec. III, knowledge of $\mathbf{F}^{(1)}$ allows the analytical evaluation of all of the coupling elements in the RPH. Second, given this information, one can subsequently step along a curved path as opposed to the linear path tangent.

These two considerations are not unrelated. If one chooses not to evaluate $\mathbf{F}^{(1)}$, then the coupling elements cannot be evaluated at the saddle point and a straight line step must be taken along the eigenvector with negative eigenvalue. At this new point, Eq. (2) is no longer indeterminate and the curvature can be calculated by Eq. (7) (or by a suitable finite difference procedure). As we show in Appendix C, this curvature will be incorrect. This is not a problem of numerical precision. The curvature (and the curvature coupling elements) evaluated on the eigenvector approach an incorrect limiting value as the saddle point is approached. Extrapolating coupling elements through the saddle point based on values calculated adjacent to the saddle point will therefore be misleading.

One can evaluate the reaction path within the local cubic approximation (LCA) to the energy at the saddle point. Although the Taylor series [Eq. (13)] cannot be summed exactly in the LCA, one can compute many path derivatives and therefore sum many terms in the series. The only modification to Eqs. (15)–(18) required in the LCA is the use of

$$F_{ij}^{(n)} = \sum_k G_{ijk}\mathbf{v}_k^{(n-1)}, \quad n > 0 \tag{21}$$

instead of Eq. (12), i.e., higher order energy derivatives are ignored.

Alternatively, if only third derivatives along the path tangent are available, then all of the $\mathbf{F}^{(n)}$ except $\mathbf{F}$ and $\mathbf{F}^{(1)}$ are set equal to zero and there will still result nonzero vectors $\mathbf{v}^{(n)}$ which will approximate the LCA values. These, too can be obtained from Eqs. (15)–(18). The reaction path near the saddle point will then be obtained by summing a number of terms in the Taylor series using these approximate LCA vectors $\mathbf{v}^{(n)}$.

C. Reaction path following

Reaction paths are usually followed using Euler based methods. Beginning at the saddle point one first steps along the path tangent [Eq. (14)] which is an eigenvector of $\mathbf{F}$. Subsequent steps are along the steepest descent direction. These steps require only first energy derivatives. If a step is too large then one can use a device based on constrained energy minimization to return to the path.[13]

If the reason for following a reaction path is to check for intervening minima or barriers, or to simply visualize how a molecule might change during a reaction, then the Euler-type methods may work very well. For the most part, however, people follow reaction paths in order to get properties such as transverse vibration frequencies which depend on second energy derivatives. We have seen earlier that the reaction path can be represented as a Taylor series expansion in the arc length and that except at the saddle point, every term in this series has nonzero values in the LQA. We seek to

use the second or higher energy derivatives whenever they are available to better follow the path.

We will now give a method which is equivalent to summing the LQA Taylor series exactly.

Pechukas[11] has pointed out that parametrizing the reaction path by its arc length is but one method of representing it. He noted that the solution to

$$\frac{d\mathbf{x}(t)}{dt} = \mathbf{g} \tag{22}$$

gives a path identical to that obtained from Eq. (2) and that Eq. (22) can be solved exactly when the energy is a quadratic function of the coordinates.

The connection between Eq. (22) and Eq. (2) can be established by noting that

$$\frac{d\mathbf{x}}{dt} = \frac{d\mathbf{x}}{ds} \frac{ds}{dt}. \tag{23}$$

For the t parametrization we have

$$dx_i = \frac{dx_i}{dt} dt \tag{24}$$

so that the arc length defined in Eq. (1) satisfies

$$\frac{ds}{dt} = \sqrt{\frac{d\mathbf{x}^\dagger}{dt} \frac{d\mathbf{x}}{dt}}, \tag{25}$$

where we have chosen the positive square root. Equation (2) is recovered by substituting Eq. (25) into Eq. (23) and then replacing $d\mathbf{x}/dt$ by $\mathbf{g}$ [Eq. (22)].

Reaction paths are followed downhill from the saddle point. For this reason we will replace $\mathbf{g}$ by $-\mathbf{g}$ in Eq. (22) in order that progress away from the saddle point be described by increasing values of t. In the LQA we begin with a point $\mathbf{x}_0 = \mathbf{x}(t=0)$, presumed to lie on the reaction path but not at the saddle point, and compute the first and second energy derivatives at that point. All higher derivatives are set equal to zero. The energy gradient in the LQA then becomes

$$\mathbf{g}(\mathbf{x}) = \mathbf{g}_0 + \mathbf{F}_0(\mathbf{x} - \mathbf{x}_0), \tag{26}$$

where $\mathbf{g}_0$ and $\mathbf{F}_0$ are, respectively, the mass weighted gradient and force constant matrix at $\mathbf{x} = \mathbf{x}_0$. Here, the subscript zero means that the quantities are evaluated at the expansion point $\mathbf{x}_0$ which is any point on the path except the saddle point.

The steepest descent path is obtained by integrating

$$\frac{d\mathbf{x}}{dt} = -\mathbf{g}_0 - \mathbf{F}_0(\mathbf{x} - \mathbf{x}_0). \tag{27}$$

It is computationally and conceptually convenient to transform Eq. (27) to generalized normal coordinates. Letting $\boldsymbol{\lambda}$ and $\mathbf{U}_0'$ be the diagonal matrix of eigenvalues and orthogonal matrix of column eigenvectors of $\mathbf{F}_0$, the solution to Eq. (27) can be written as

$$\mathbf{x}(t) = \mathbf{x}_0 + \mathbf{A}(t)\mathbf{g}_0, \tag{28}$$

where

$$\mathbf{A}(t) = \mathbf{U}_0'\boldsymbol{\alpha}(t)\mathbf{U}_0'^\dagger. \tag{29}$$

$\boldsymbol{\alpha}(t)$ is a diagonal matrix whose elements are given as

$$\alpha_{ii} = (e^{-\lambda_{ii}t} - 1)/\lambda_{ii}$$
$$\approx -t + \tfrac{1}{2}\lambda_{ii}t^2 - \tfrac{1}{6}\lambda_{ii}^2 t^3 + \cdots. \tag{30}$$

The series form is useful when t is very small. We note that an equation essentially identical to Eq. (28) has been used by Camp and King as part of a strategy for optimizing MCSCF wave functions with respect to orbital rotations.[15]

The relationship between the parameter t and the arc length along the curved LQA path can be obtained from Eq. (25). In order to bring this into a computationally useful form we first substitute Eq. (28) into the right-hand side of Eq. (27) and multiply the resulting equation on the left by $\mathbf{U}_0'^\dagger$ to get

$$\frac{d\mathbf{x}'}{dt} = \mathbf{U}_0^\dagger \frac{d\mathbf{x}}{dt} = -(\boldsymbol{\lambda}\mathbf{A}' + \mathbf{I})\mathbf{g}_0', \tag{31}$$

where

$$\mathbf{g}_0' = \mathbf{U}_0'^\dagger\mathbf{g}_0 \tag{32}$$

is the gradient in generalized normal coordinates. Using the fact that $\mathbf{x}'^\dagger\mathbf{x}' = \mathbf{x}^\dagger\mathbf{x}$, Eq. (25) becomes, upon substitution of Eq. (31),

$$\frac{ds}{dt} = \left\{ \sum_i g_{0,i}'^2 \, e^{-2\lambda_{ii}t} \right\}^{1/2}. \tag{33}$$

Given any step size in the arc length, Eq. (33) can be numerically integrated using small steps in t until the desired arc length is reached. The corresponding value of t is then used in Eq. (28) to give the path coordinates that result from the chosen arc length. The numerical integration of Eq. (33) consumes negligible computer time because no new energy derivatives are required.

Figures 1, 2, and 3 illustrate the differences between the LQA path, the Euler path, and the exact path on the model
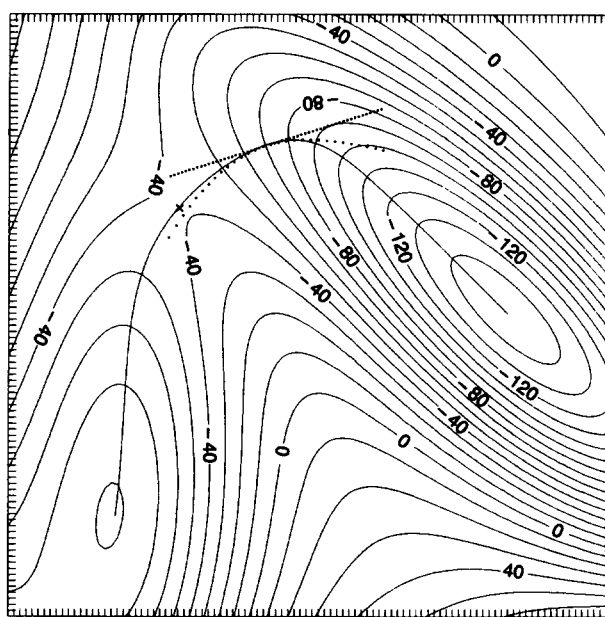

FIG. 1. Comparison of reaction paths based on a local linear approximation to the energy (straight path) and a local quadratic approximation (LQA) to the energy (curved path). The true reaction path is represented by a solid line. The point of expansion is the intersection of the reaction path with the -70 contour. The potential function for all of the figures is the Muller–Brown function [Ref. 8(b)].
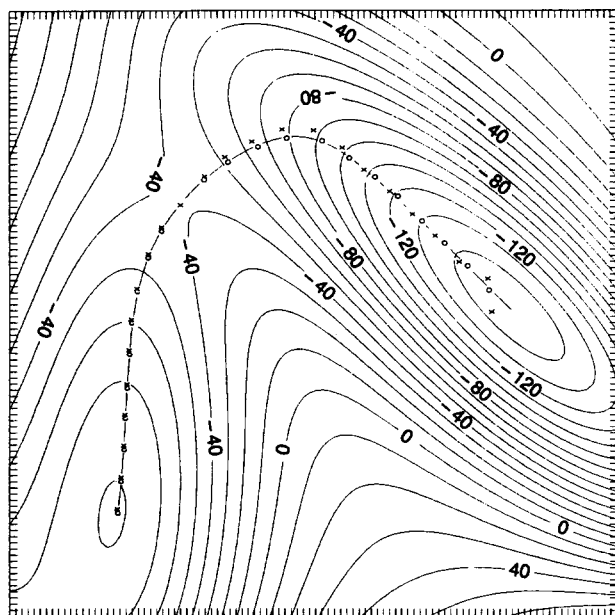
FIG. 2. Comparison of Euler method (×'s) and LQA method (circles) for following the reaction path. Note the deviation of the Euler path from the true reaction path in the region of large curvature.

two-dimensional potential surface of Muller and Brown.[8(b)] In Fig. 1 the paths generated at the same expansion point are compared. The curved nature of the LQA path is evident. Figures 2 and 3 show the complete reaction paths for two different step sizes. In each case, the Euler path is initiated along the eigenvector with negative curvature and the LQA path is initiated along a curved path using the first three terms of the Taylor series [Eq. (13)]. We note the stability of the LQA path in Fig. 3. The LQA path smoothly rejoins the exact reaction path near products whereas the linear Euler path displays its characteristic zig–zag pattern.
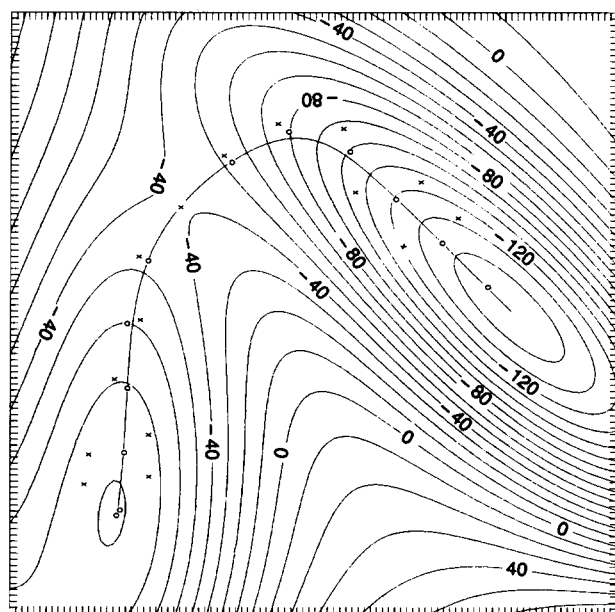
As discussed earlier, two-dimensional plots of reaction paths do not fully illustrate the fact that the LQA path approximately accounts not only for curvature but for twisting in all dimensions. This is in contrast to the Euler method which is one dimensional or a three term Taylor series, which is two dimensional.

It appears from Figs. 2 and 3 that all methods represent the reaction path near the saddlepoint reasonably well. This is misleading. Figure 4 shows the scalar curvature $\kappa(s)$ [Eq. (6)] calculated at each step along the reaction path for two step sizes differing by an order of magnitude. In each case, the path is initiated along the eigenvector with negative eigenvalue and the LQA method is used for subsequent steps. In this two-dimensional case, $\kappa(s)$ can also be regarded as one of the curvature coupling elements in the RPH. Note the large deviations from the exact values near the saddle point. The curvature formula is exact and we have verified that there is no numerical precision difficulty is evaluating the formula. The deviations must therefore be due to imprecisions in determining the path itself. Note also that as the step size is decreased the curvature appears to approach a smooth curve through the saddle point region, except for the poor values at the first steps. Figure 5 displays the same curve as Fig. 4 generated by first calculating the correct curvature at the saddle point [Eq. (19)] and taking a first step along the curved path instead of along the eigenvector. This results in qualitatively correct behavior even for fairly large step sizes.

In Appendix C it is shown that as the saddle point is approached along the sequence of points which lie on an eigenvector of F evaluated at the saddle point, the curvature vector calculated by Eq. (7) tends toward a value that is
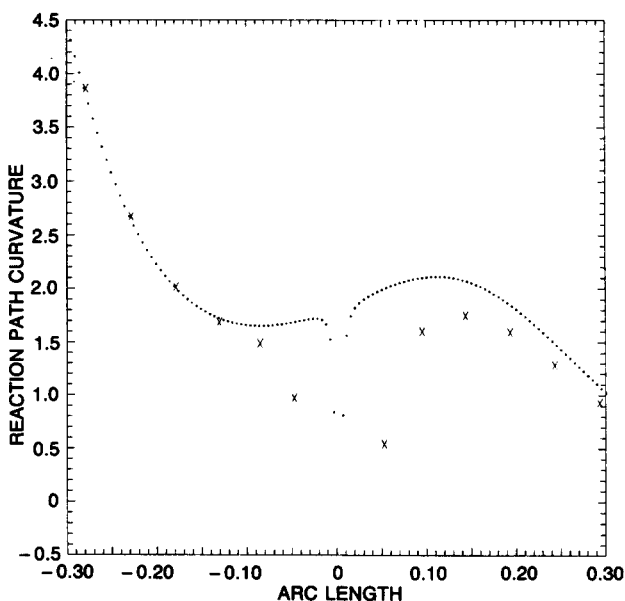

FIG. 4. Calculated curvature of the steepest descent reaction path as a function of arc length. The path is initiated from the saddle point along the eigenvector with negative curvature. For subsequent steps the LQA algorithm is used. The ×'s refer to a step size of 0.05 and the circles refer to a step size of 0.005. The region shown extends about one-third of the way toward the reactant and product wells.

FIG. 3. Same as Fig. 2 with a larger step size for following the path. Note the characteristic zig–zag behavior of the Euler method.
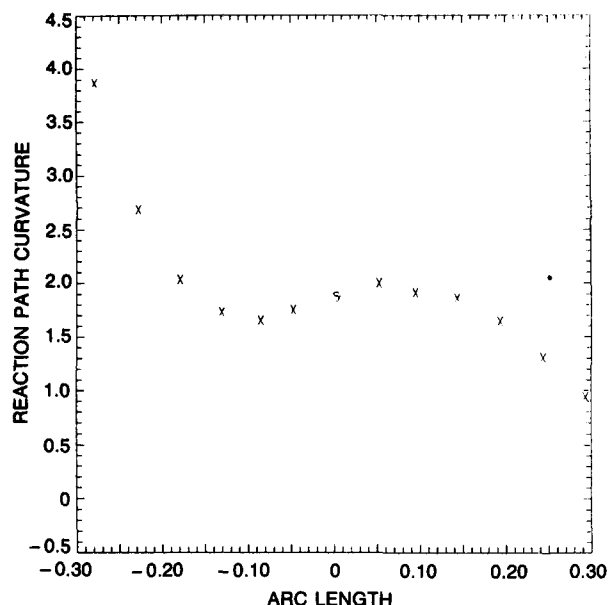
FIG. 5. Same as Fig. 4 except that the curvature is calculated correctly at the saddle point and the first step is along a curved path toward reactants and products, step size = 0.05.

different from the correct limiting value. This accounts for the behavior shown in Fig. 4. The very first step along the path tangent **v** gives an incorrect curvature, regardless of how small a step size is used. The true reaction path is a curved path. At the saddle point the curvature is due to non-zero third energy derivatives. If one chooses the path to lie along the straight line defined by the second energy derivatives alone then there will always be a deviation.

A solution to this problem is to leave the saddle point along a curved path. As described in the previous section this can be done by representing the path as a Taylor series expansion in the LCA or the approximate LCA obtained by retaining only $\mathbf{F}^{(1)}$. This requires the third energy derivatives, but at least some of them must be calculated in order to evaluate the curvature at the saddle point itself.

In *ab initio* calculations the curvature at the saddle point is sometimes obtained by interpolating between values calculated on either side. Figure 4 suggests, however, that apparently reasonable interpolations can lead to significant errors.

We show in the next section that in order to evaluate all of the RPH coupling parameters, $\mathbf{F}^{(1)}$ is needed at every point on the reaction path. This information can be used to better follow the reaction path at nonstationary points. The simplest way[16] of doing this is to approximate the LCA path by computing a large number of terms in the Taylor series expansion, Eq. (13). Since the steepest descent direction is used, the right-hand sides of Eqs. (2) and (10) should be replaced by their negatives. In the local cubic approximation where all the third derivatives are available, $\mathbf{F}^{(n)}$ is given by Eq. (21), and by

$$\mathbf{F}^{(n)} = \delta_{1n}\mathbf{F}^{(1)}, \qquad (34)$$

when only $\mathbf{F}^{(1)}$ is available.

III. THE RPH PARAMETERS

The essential idea underlying the RPH is the replacement of the $3N$ mass weighted Cartesian displacement coordinates of the atoms by $3N$ coordinates consisting of displacement along the reaction path, three translations, three rotations, and $3N - 7$ eigenvectors of the projected force constant matrix

$$\mathbf{K}(s) = [\mathbf{I} - \mathbf{P}(s)]\mathbf{F}(s)[\mathbf{I} - \mathbf{P}(s)] \qquad (35)$$

described by Miller, Handy, and Adams.[1] We have formally included the parametric dependence of the force constant matrix $\mathbf{F}$ and the projection matrix $\mathbf{P}$ on s to emphasize that these matrices are to be evaluated at a point $\mathbf{x}(s)$ which lies on the reaction path, and that they change as s changes.

The parameters of the RPH described in the next few subsections involve quantities that look like changes in normal mode eigenvalues and eigenvectors with respect to a displacement along the reaction path. These changes can be thought of as the sum of two contributions: changes due to the changes in the force constant matrix $\mathbf{F}$ due to nonzero third energy derivatives and changes due to changes in the projection matrix $\mathbf{P}$. In the LQA only the latter contribution survives. As one moves along the LQA reaction path, the normal mode eigenvalues and eigenvectors of $\mathbf{K}$ must change in order to remain orthogonal to the curving path. In addition, they must change in order to remain orthogonal to the changing subspace which corresponds to overall molecular rotations.

A. The projection matrix P

Evaluation of the RPH coupling parameters requires the projection matrix $\mathbf{P}$ and its derivative $d\mathbf{P}/ds$. Miller, Handy, and Adams[1] give explicit formulas for evaluating $\mathbf{P}$. In Appendix D we present an alternative construction of $\mathbf{P}$ which is easily differentiated with respect to arc length to give a simple analytical formula for $d\mathbf{P}/ds$.

B. Changes in transverse vibrations

At any point on the reaction path, the $3N - 7$ transverse vibrational modes $\mathbf{L}_i$ are obtained as orthonormal eigenvectors of the projected mass weighted force constant matrix $\mathbf{K}(s)$:

$$\mathbf{K}(s)\mathbf{L}_i(s) = \omega_i^2(s)\mathbf{L}_i(s), \qquad (36)$$

where the eigenvalue $\omega_i^2(s)$ is the square of the corresponding transverse frequency. The set of eigenvectors of $\mathbf{K}$ are completed by adding the six translations and rotations $\mathbf{v}_i(s)$ and the reaction path tangent $\mathbf{v}(s)$, all seven of which have corresponding eigenvalues equal to zero.

At a nearby point on the path the $\mathbf{L}_i$ will have changed due to the fact that $\mathbf{K}$ has changed,

$$\mathbf{L}_i(s + \delta s) \approx \mathbf{L}_i(s) + \delta s \frac{\partial \mathbf{L}_i}{ds}. \qquad (37)$$

The new $\mathbf{L}_i(s + \delta s)$ can be resolved into its components along the $3N$ eigenvectors of $K(s)$,

$$\mathbf{L}_i(s + \delta s)$$

$$\approx \mathbf{L}_i(s) + \delta s \left(\sum_{j \neq i}^{3N-7} B_{i,j}(s) \mathbf{L}_j(s) + \sum_{j=1}^{6} B_{i,3N-7+j} \mathbf{v}_i(s) \right.$$

$$\left. + B_{i,3N}(s) \mathbf{v}(s) \right). \tag{38}$$

The $B_{i,j}$ are the RPH coupling constants, formulas for which are obtained by differentiating Eq. (36), multiplying the result by $\mathbf{L}_j^\dagger$ and solving for $\mathbf{L}_j^\dagger(d\,\mathbf{L}_i/ds)$, a procedure identical to first order perturbation theory,

$$B_{i,j} = \mathbf{L}_j^\dagger \frac{d\mathbf{L}_i}{ds} = \frac{\mathbf{L}_j^\dagger(d\mathbf{K}/ds)\mathbf{L}_i}{\omega_i^2 - \omega_j^2}, \quad \begin{matrix} i = 1,3N-7, \\ j = 1,3N-7, \\ j \neq i, \end{matrix} \tag{39}$$

$$B_{i,3N-7+j} = \mathbf{v}_j^\dagger \frac{d\mathbf{L}_i}{ds} = \frac{\mathbf{v}_j^\dagger(d\mathbf{K}/ds)\mathbf{L}_i}{\omega_i^2}, \quad \begin{matrix} i = 1,3N-7, \\ j = 1,6, \end{matrix} \tag{40}$$

$$B_{i,3N} = \mathbf{v}^\dagger \frac{d\mathbf{L}_i}{ds} = \frac{\mathbf{v}^\dagger(d\mathbf{K}/ds)\mathbf{L}_i}{\omega_i^2}, \quad i = 1,3N-7. \tag{41}$$

The transverse frequencies also change with motion along the reaction path

$$\omega_i^2(s + \delta s) \approx \omega_i^2(s) + \frac{d\omega_i^2}{ds} \delta s, \tag{42}$$

where

$$\omega_i^2 = \mathbf{L}_i^\dagger \mathbf{K} \mathbf{L}_i = \mathbf{L}_i^\dagger(\mathbf{I} - \mathbf{P})\mathbf{F}(\mathbf{I} - \mathbf{P})\mathbf{L}_i = \mathbf{L}_i^\dagger \mathbf{F} \mathbf{L}_i. \tag{43}$$

The derivative $d\omega_i^2/ds$ is also important in the RPH. It too can be evaluated by first order perturbation theory,

$$\frac{d\omega_i^2}{ds} = \mathbf{L}_i^\dagger \frac{d\mathbf{K}}{ds} \mathbf{L}_i. \tag{44}$$

In order to facilitate the evaluation of the right-hand sides of Eqs. (39), (40), and (41) and also to aid in their interpretation, we differentiate Eq. (35) and then divide $d\mathbf{K}/ds$ into the sum of two contributions:

$$\frac{d\mathbf{K}}{ds} = \mathbf{K}'_{LQA}(s) + (\mathbf{I} - \mathbf{P}) \frac{d\mathbf{F}}{ds}(\mathbf{I} - \mathbf{P}), \tag{45}$$

where

$$\mathbf{K}'_{LQA} = -\frac{d\mathbf{P}}{ds}\mathbf{F}(\mathbf{I} - \mathbf{P}) - (\mathbf{I} - \mathbf{P})\mathbf{F}\frac{d\mathbf{P}}{ds} \tag{46}$$

involves only second energy derivatives (at nonstationary points). It reflects changes in $\mathbf{K}$ due to the changing rotations and path tangent which are projected out. Analytical formulas for $\mathbf{P}$ and $d\mathbf{P}/ds$ are given in Eqs. (D1) and (D14). The second term in Eq. (45) is proportional to third energy derivatives and is independent of changes in the rotations and path tangent. Since these are annihilated by $(\mathbf{I} - \mathbf{P})$, any matrix element over $d\mathbf{K}/ds$ involving a translation, rotation, or path tangent will have no contribution from third energy derivatives. These matrix elements will be computed exactly in the LQA.

At this stage we point out that all the formulas required to evaluate the RPH parameters analytically given the geometry and first, second, and some third energy derivatives at a point on the reaction path have now been derived. Equations (2) and (7) [or Eqs. (14) and (19) at the saddle

point] give the path tangent and curvature, respectively; the coupling parameters are obtained from Eqs. (39) and (41) and the frequency parameters, $-\frac{1}{2}\omega_i (d\omega_i/ds)$ are obtained from ω_i^2 and $(d\omega_i^2/ds)$, Eqs. (43) and (44), as

$$-\frac{1}{4\omega_i^2}\frac{d\omega_i^2}{ds}.$$

However, deeper insight into the nature of these couplings can be gained from more detailed examination of the formalism. This is done in the following three subsections.

C. Coupling of transverse vibrations to the reaction path

A coupling of transverse modes to the reaction path arises through the curvature of the reaction path. The curvature coupling elements in the RPH are in fact elements of the reaction path curvature vector expressed in a basis of generalized normal mode eigenvectors. These coupling elements can be evaluated from Eq. (41) or, alternatively, from the orthogonality relation

$$B_{i,3N} = \mathbf{v}^\dagger \frac{d\mathbf{L}_i}{ds} = -\mathbf{L}_i^\dagger \frac{d\mathbf{v}}{ds}, \tag{47}$$

where the curvature vector $d\mathbf{v}/ds$ is given by Eq. (7). This leads to

$$B_{i,3N} = -\mathbf{L}_i^\dagger \mathbf{F} \mathbf{v}/c, \tag{48}$$

where $\mathbf{v}$ is given by Eq. (2) for the reactant, or steepest ascent, branch or by its negative for the product, or steepest descent, branch. The sign of $\mathbf{L}_i$ is arbitrary, but should be chosen such that $\mathbf{L}_i$ is a continuous function of s.

At the saddle point, Eq. (19) should be used for $d\mathbf{v}/ds$. Using this, Eq. (47) becomes

$$B_{i,3N} = -\mathbf{L}_i^\dagger(2\mathbf{v}^\dagger \mathbf{F} \mathbf{v} \mathbf{I} - \mathbf{F})^{-1}\left(\frac{d\mathbf{F}}{ds} - \mathbf{v}^\dagger \frac{d\mathbf{F}}{ds}\mathbf{v}\mathbf{I}\right)\mathbf{v}. \tag{49}$$

At any nonstationary point on the reaction path, the curvature coupling elements are thus given simply as matrix elements over the unprojected force constant matrix. They are completely determined from second energy derivatives alone. In contrast, Eq. (48) is invalid at the saddle point and the curvature coupling elements must be determined from Eq. (49) which requires limited third derivative information.

We note from Eq. (48) or from Eq. (7), that if the reaction path tangent $\mathbf{v}$ is an eigenvector of the unprojected force constant matrix, then the curvature of the reaction path vanishes (as do all of the curvature coupling elements). This is the gradient extremal condition discussed by Ruedenberg.[14] The gradient extremal condition is equivalent to the curved reaction path being at a point of inflection, and implies a local dynamical decoupling of the reaction path from the transverse degrees of freedom.[17] Since the reaction path tangent is shown to be an eigenvector of the force constant matrix at the saddle point, it is tempting to suggest that the gradient extremal condition becomes satisfied in the vicinity of the saddle point when approaching it along the reaction path. This is not true. As long as third energy derivatives are nonzero at the saddle point, the reaction path tangent will

immediately veer away from the eigenvector of the force constant matrix as one steps off the saddle point.

D. Mode–mode couplings

The coupling between two transverse vibrational modes is given by Eq. (39). Rearranging this expression and substituting Eqs. (45) and (46) for $d\mathbf{K}/ds$ gives

$$(\omega_i^2 - \omega_j^2)B_{ij} = \mathbf{L}_j^\dagger \frac{d\mathbf{K}}{ds} \mathbf{L}_i = \mathbf{L}_j^\dagger \frac{d\mathbf{F}}{ds} \mathbf{L}_i$$

$$- \mathbf{L}_j^\dagger \frac{d\mathbf{P}}{ds} \mathbf{F}\mathbf{L}_i - \mathbf{L}_j^\dagger\mathbf{F}\frac{d\mathbf{P}}{ds}\mathbf{L}_i, \qquad (50)$$

where $d\mathbf{P}/ds$ is given by Eq. (D14). The first term is the contribution from the component of the third derivatives along the path tangent. The remaining two terms are the contributions due to the separate couplings of $\mathbf{L}_i$ and $\mathbf{L}_j$ to the translations, rotations, and path tangent. This can be seen more clearly by writing $d\mathbf{P}/ds$ in terms of orthonormal translation–rotation vectors:

$$\frac{d\mathbf{P}}{ds} = \sum_{k=1}^{7} \left(\mathbf{v}_k \frac{d\mathbf{v}_k^\dagger}{ds} + \frac{d\mathbf{v}_k}{ds} \mathbf{v}_k^\dagger \right), \qquad (51)$$

where $\mathbf{v}_7 = \mathbf{L}_{3N} = \mathbf{v}$. Equation (50) then becomes

$$(\omega_i^2 - \omega_j^2)B_{ij} = \mathbf{L}_j^\dagger \frac{d\mathbf{F}}{ds} \mathbf{L}_i - \sum_{k=1}^{7} (B_{3N-6+k,j}\mathbf{v}_k^+\mathbf{F}\mathbf{L}_i$$

$$+ B_{3N-6+k,i}\mathbf{v}_k^\dagger\mathbf{F}\mathbf{L}_j), \qquad (52)$$

where

$$B_{3N-6+k,i} = \frac{d\mathbf{v}_k^\dagger}{ds} \mathbf{L}_i = -\frac{d\mathbf{L}_i^\dagger}{ds} \mathbf{v}_k \qquad (53)$$

are the couplings between $\mathbf{L}_i$ and the translations, rotations, and path tangent. Note that in the LQA ($d\mathbf{F}/ds = 0$), the mode–mode couplings are still nonzero due to these separate couplings of $\mathbf{L}_i$ and $\mathbf{L}_j$ to the translations, rotations, and path tangent.

At the saddle point, only the first term of Eq. (52) survives. This is not because the couplings to the translations, rotations, and path tangent are zero, for they are not. Rather it is due to the fact that the eigenvectors of $\mathbf{K}$ are also eigenvectors of $\mathbf{F}$ so that off-diagonal elements of the form $\mathbf{v}_k^\dagger\mathbf{F}\mathbf{L}_i$ are equal to zero.

E. Diagonal couplings

The diagonal elements of $B_{i,j} = (d\mathbf{L}_i^\dagger/ds)\mathbf{L}_j$ are identically zero because of the fact that $\mathbf{L}_i$ is normalized for all s. When the classical RPH is transformed to the harmonic action-angle variables, terms involving the transverse-frequency derivatives appear. It is customary to define the diagonal coupling elements to be these terms[1]:

$$B_{ii} = -\frac{1}{2\omega_i} \frac{d\omega_i}{ds} = -\frac{1}{4\omega_i^2} \frac{d\omega_i^2}{ds}. \qquad (54)$$

Using Eqs. (44), (45), and (46) and rearranging gives

$$- 4\omega_i^2 B_{ii} = \mathbf{L}_i^\dagger \frac{d\mathbf{F}}{ds} \mathbf{L}_i - \mathbf{L}_i^\dagger\left(\frac{d\mathbf{P}}{ds}\mathbf{F} + \mathbf{F}\frac{d\mathbf{P}}{ds}\right)\mathbf{L}_i \qquad (55)$$

in close analogy to Eq. (50) for the off-diagonal couplings.

Similar to Eq. (50) the second term in Eq. (55) also vanishes at the saddle point.

IV. SUMMARY AND CONCLUSIONS

The complete evaluation of the RPH consists of three distinct steps: (1) Locate the saddle point for the reaction, (2) determine the reaction path, and (3) compute the RPH parameters at selected points along the path. In this paper we have derived analytic formulas that are relevant to the second and third steps. For the most part, it is not advocated that anything new be calculated, simply that available information be utilized to the fullest extent.

Given the gradient of the energy and the matrix of second derivatives, $\mathbf{F}$, at some nonstationary point on the reaction path, e.g., a calculation can proceed as follows. The reaction path tangent, $\mathbf{v}$ is constructed as the normalized energy gradient. Knowledge of the path tangent in conjunction with the molecular geometry in Cartesian coordinates and the atomic masses are then used to construct the projection matrix $\mathbf{P}$. The projected force constant matrix $\mathbf{K}$, formed from $\mathbf{F}$ and $\mathbf{P}$, is then diagonalized to give the generalized normal modes $\mathbf{L}_i$ and the corresponding frequencies ω_i^2. The curvature of the reaction path, expressed in Cartesian coordinates can be evaluated from $\mathbf{F}$ and $\mathbf{v}$. The normal mode eigenvectors can then be used to calculate the RPH curvature coupling elements.

For some dynamical models, or for qualitative studies of energy transfer, this is all the information that is required. In other applications, one also seeks to calculate the mode–mode coupling elements and the diagonal (frequency derivative) coupling elements. These can be approximately evaluated using the above information (i.e., within the LQA). These coupling elements involve changes in normal mode eigenvectors and eigenvalues along the reaction path. These eigenvectors change with arc length s for two reasons. The first is that the normal mode eigenvectors are required to remain orthogonal to the reaction path tangent and (through the projection matrix) to the vectors corresponding to overall molecular rotations. Since the rotation derivatives depend only on geometry and atomic masses, and the reaction path curvature is known, this portion is correctly evaluated within the LQA. The second reason these eigenvectors change is that $\mathbf{F}$ itself changes with s due to nonzero third energy derivatives. This effect is absent within the LQA.

Finally, the force constant matrix can be used to help follow the reaction path. Knowledge of the reaction path curvature suggests a Taylor series representation of the path carried to third order. One can, in fact, do better than this. Within the LQA, this series representation of the path is correct through third order, but has a nonzero contribution at all orders. Summing this series to all orders is equivalent to solving the differential equation for the steepest descent path within the LQA which is easily done. The resulting LQA path is not only a curved path, but like the true reaction path it twists (like a corkscrew) through the many-dimensional space.

If one wishes to calculate the mode–mode and frequency derivative coupling constants exactly, then limited third

energy derivative information is required. The required matrix is the Cartesian third derivatives contracted with the reaction path tangent, or alternatively, the force constant matrix differenced along the reaction path. In calculating these coupling constants, it is advised that the LQA portion be evaluated analytically, and the differencing be limited to the third derivative contribution. This is in contrast to differencing generalized normal mode eigenvectors which is equivalent to differencing both the second order and third order contributions to the coupling constants.

If the mode–mode and diagonal coupling elements have been calculated, then the limited third derivative information mentioned above can also be used for the following the path. The differential equation defining the path cannot be solved in this case, but the Taylor series representation of the path can be summed to arbitrary order by a straightforward algorithm.

The saddle point on the potential energy surface requires special consideration. In the vicinity of the saddle point, the norm of the gradient vector approaches zero and its direction becomes undefined. One therefore expects to have numerical difficulties as these quantities begin to approach the resolution of the calculation procedure. We have shown that the difficulties are in fact more insidious than this. The computed RPH parameters are always slightly incorrect if one is not exactly on the reaction path, but this difficulty becomes more profound in the vicinity of the stationary point. In fact, if one steps off the saddle point on the tangent to the reaction path and computes the curvature coupling elements at the new point, these elements will be incorrect. This is true regardless of the step size and regardless of the numerical precision. In order to correctly calculate the curvature adjacent to the saddle point, one must leave the saddle point on a curved path.

Equations valid at the saddle point were obtained by a limiting procedure based on L 'Hospital's rule. At the saddle point, second derivatives are required simply to define the path tangent, in contrast to first derivatives at nonstationary points. We have also shown that third derivatives are required to obtain the reaction path curvature and the curvature coupling constants at the saddle point. This limited third derivative information (the same as that described above) is also sufficient to exactly compute all of the coupling constants at the saddle point. Given these third energy derivatives at the saddle point, one can evaluate a few or several terms in the series representation of the reaction path to generate a subsequent step toward reactant or product.

In summary, we have shown that the same information is required at any point on the reaction path if one wishes to evaluate the entire RPH. This includes the Cartesian coordinates of the atoms, the atomic masses, the potential energy, the energy gradient, the matrix of second derivatives, and limited third derivatives (second derivatives differenced along the reaction path direction). We have shown how all of this information can be straightforwardly used to help map out the reaction path.

ACKNOWLEDGMENT

APPENDIX A: DERIVATION OF $v^{(n)}$ AT NONSTATIONARY POINTS

We begin by rewriting Eq. (2) as

$$c v = \pm \mathbf{g}, \tag{A1}$$

where c is given by Eq. (4). The positive sign is used for steepest ascent paths and the negative for steepest descent paths.

We differentiate Eq. (A1) n times to get

$$\frac{d^n c v}{ds^n} = \pm \mathbf{g}^{(n)}. \tag{A2}$$

The left-hand side of Eq. (A2) can be written as a binomial expansion,

$$\frac{d^n c v}{ds^n} = \sum_{k=0}^{n} \binom{n}{k} c^{(n-k)} v^{(k)} \tag{A3}$$

$$= c v^{(n)} \pm Q(n), \tag{A4}$$

where

$$Q(n) = \pm \sum_{k=0}^{n-1} \binom{n}{k} c^{(n-k)} v^{(k)} = \pm \sum_{k=1}^{n-1} \binom{n}{k} c^{(k)} v^{(n-k)}. \tag{A5}$$

The form [Eq. (A4)] has completely isolated $v^{(n)}$ as we show below.

The derivatives of c can also be written as a binomial expansion. We first note that the equation for $c^{(1)}$ is, by differentiating Eq. (4) and using Eq. (9),

$$c^{(1)} = \pm v^\dagger F v. \tag{A6}$$

Differentiating this equation, i times gives

$$c^{(i+1)} = \pm \sum_{l=0}^{i} \binom{i}{l} v^{(i-l)\dagger} \left(\frac{d^l (F v)}{ds^l} \right)$$

$$= \pm \sum_{l=0}^{i} \binom{i}{l} v^{(i-l)\dagger} \left(\sum_{m=0}^{l} \binom{l}{m} F^{(l-m)} v^{(m)} \right)$$

$$= \pm \sum_{l=0}^{i} \sum_{m=0}^{l} \binom{i}{l}\binom{l}{m} v^{(i-l)\dagger} F^{(l-m)} v^{(m)}, \tag{A7}$$

where the dagger refers to the steepest ascent branch [Eq. (11)].

We note that the highest derivative of c that appears in Eq. (A5) is $c^{(n)}$. From Eq. (A7) with $i + 1 = n$ we see that the highest derivative of v that appears is $v^{(n-1)}$. Similarly we also note that the highest derivative of F that appears in $c^{(n)}$ is $F^{(n-1)}$, which from Eq. (12) depends at most on $v^{(n-2)}$. Therefore, the sum in Eq. (A5) depends at most on $v^{(n-1)}$ so that $v^{(n)}$ is completely isolated in Eq. (A4).

We now differentiate the right-hand side of Eq. (A1) n times,

$$\pm \mathbf{g}^{(n)} = \pm \frac{d^n \mathbf{g}}{ds^n} = \pm \frac{d^{n-1} F v}{ds^{n-1}}$$

$$= \pm \sum_{k=0}^{n-1} \binom{n-1}{k} F^{(n-1-k)} v^{(k)}, \tag{A8}$$

where we have used Eq. (9). By arguments similar to those of the above paragraph we see that $v^{(n-1)}$ is the highest derivative of v that appears in Eq. (A8).

The final result is obtained by substituting Eq. (A4) and Eq. (A8) into Eq. (A2) and solving for $\mathbf{v}^{(n)}$,

$$\mathbf{v}^{(n)} = c^{-1} \sum_{k=0}^{n-1} \left[\pm \binom{n-1}{k} \mathbf{F}^{(n-1-k)} - \binom{n}{k} c^{(n-k)} \mathbf{I} \right] \mathbf{v}^{(k)}. \tag{A9}$$

The right-hand side of Eq. (A9) depends at most on $\mathbf{v}^{(n-1)}$.

It is helpful to clarify the signs in Eq. (A9), i.e., the steepest descent form vs the steepest ascent form. This is most easily done by substituting Eq. (A7) into Eq. (A9) to obtain the expanded form

$$\mathbf{v}^{(n)} = \pm c^{-1} \left\{ \sum_{k=0}^{n-1} \binom{n-1}{k} \mathbf{F}^{(n-1-k)} \mathbf{v}^{(k)} \right. $$
$$ - \mathbf{I} \sum_{k=0}^{n-1} \binom{n-1}{k} \sum_{l=0}^{n-k-1} $$
$$ \times \sum_{m=0}^{l} \binom{n-k-1}{l} \binom{l}{m} $$
$$ \left. \times \mathbf{v}^{(n-k-1-l)\dagger} \mathbf{F}^{(l-m)} \mathbf{v}^{(m)} \mathbf{v}^{(k)} \right\}. \tag{A10}$$

Although not computationally useful, this form shows that the formulas for the steepest descent vectors are just the opposite signs of those for the steepest ascent vectors. This does not mean that the values of the vectors are opposite. In fact, by simply replacing ds by $-ds$ everywhere we see that $\mathbf{v}^{(n)}$ (steepest descent) equals $\mathbf{v}^{(n)}$ (steepest ascent) if n is odd and equals $-\mathbf{v}^{(n)}$ (steepest ascent) if n is even.

APPENDIX B: DERIVATION OF $\mathbf{v}^{(n)}$ AT THE SADDLE POINT

We begin by borrowing from the results of Appendix A. Substituting Eq. (A4) into Eq. (A2) we have

$$c\mathbf{v}^{(n)} \pm \mathbf{Q}(n) = \pm \mathbf{g}^{(n)}, \tag{B1}$$

where $\mathbf{Q}(n)$ is given by Eq. (A5) when $n > 0$. Using Eq. (A7), this can be written as

$$\mathbf{Q}(n) = \sum_{k=1}^{n-1} \sum_{l=0}^{k-1} \sum_{m=0}^{l} \binom{n}{k} \binom{k-1}{l} \binom{l}{m}$$
$$ \times \mathbf{v}^{(k-1-l)\dagger} \mathbf{F}^{(l-m)} \mathbf{v}^{(m)} \mathbf{v}^{(n-k)}, \quad n > 0 \tag{B2}$$

and from Eq. (A2),

$$\mathbf{Q}(0) = 0. \tag{B3}$$

The formula for $\mathbf{g}^{(n)}$ is given in Eq. (A8). We rearrange Eq. (B1) to give

$$c\mathbf{v}^{(n)} = \pm [\mathbf{g}^{(n)} - \mathbf{Q}(n)], \tag{B4}$$

and note from Appendix A that the right-hand side of Eq. (B4) depends at most on $\mathbf{v}^{(n-1)}$ and energy derivatives. For example, taking $n = 1$ we have

$$c\mathbf{v}^{(1)} = \pm [\mathbf{Fv} - (\mathbf{v}^\dagger \mathbf{Fv})\mathbf{v}] \tag{B5}$$

using Eqs. (11) and (B2). We wish to examine the behavior of Eq. (B4) as the saddle point is approached.

Since $\mathbf{g}$ and hence c approach zero as the saddle point is approached, we see from Eq. (B4) that $\mathbf{v}^{(n)}$ has a finite value at the saddle point if

$$\lim_{s \to 0} c\mathbf{v}^{(n)} = \pm [\mathbf{g}_0^{(n)} - \mathbf{Q}_0(n)] = 0, \tag{B6}$$

where $\mathbf{g}_0^{(n)}$ and $\mathbf{Q}_0(n)$ are the limiting values of these quantities [Eqs. (A8) and (B2)] at the saddle point.

Equation (B6) is the fundamental equation for determining the limiting values of the path derivatives as the saddle point is approached along the path. If $\mathbf{g}^{(n)} = \mathbf{Q}_0(n)$ then not only are we assured of a finite value for $\mathbf{v}_0^{(n)}$ but this equation can be solved for $\mathbf{v}_0^{(n-1)}$. We only need to determine that the solution is unique in order to show, by induction, that all $\mathbf{v}_0^{(n)}$ are finite and uniquely determined by Eq. (B6).

Equation (B6) is equivalent to using L 'Hospital's rule to obtain $\mathbf{v}_0^{(n-1)}$, the limiting value of $\mathbf{v}^{(n-1)}$ as the saddle point is approached along the reaction path. Consider, e.g., the path tangent $\mathbf{v}^{(0)}$. Applying L 'Hospital's rule to Eq. (2) gives

$$\mathbf{v}_0 = \lim_{s \to 0} \frac{\mathbf{g}(s)}{c(s)} = \left(\frac{d\mathbf{g}}{ds} \right)_{s=0} \Big/ \left(\frac{dc}{ds} \right)_{s=0}. \tag{B7}$$

If the approach to the saddle point is taken to be along $d\mathbf{x}/ds = \mathbf{v}$ then we obtain Eq. (14) by substituting Eqs. (A6) and (A8) (for $n = 1$) into Eq. (B7) and rearranging. We recognize Eq. (14) to be the right-hand side of Eq. (B5) evaluated at the saddle point. Since this is zero [by Eq. (14)], Eq. (B6) shows that $\mathbf{v}^{(1)}$ has a finite value at the saddle point.

Equation (14) has only one solution (the eigenvector corresponding to the single negative eigenvalue of $\mathbf{F}$ evaluated at the saddle point) that is consistent with the definition of the reaction path. Hence $\mathbf{v}_0$ is uniquely determined as a solution to $\mathbf{g}_0^{(1)} = \mathbf{Q}_0(1)$ which, as we have seen, is equivalent to determining $\mathbf{v}_0$ by L 'Hospital's rule. In the same way, it is not difficult to show that, in general, solving

$$\mathbf{g}_0^{(n+1)} = \mathbf{Q}_0(n+1) \tag{B8}$$

for $\mathbf{v}_0^{(n)}$ is equivalent to determining it by applying L 'Hospital's rule to Eq. (B4).

The solution [Eq. (15)] is obtained by replacing n by $n + 1$ in Eqs. (A8) and (B2) and then substituting them into Eq. (B8) and solving for $\mathbf{v}_0^{(n)}$. The solution for $n > 1$ is unique because the matrix $\mathbf{M}(n)$ defined in Eq. (16) has no zero eigenvalues.

APPENDIX C: BEHAVIOR OF THE PATH CURVATURE NEAR THE SADDLE POINT

In Appendix B we derived the correct limiting values of the path derivatives $\mathbf{v}_0^{(n)}$ as the saddle point is approached along the reaction path. In this Appendix we investigate the behavior of the curvature vector $\mathbf{v}^{(1)}$ as the saddle point is approached along a different path, namely along the eigenvector of $\mathbf{F}_0$, the force constant matrix at the saddle point, that corresponds to the single negative eigenvalue.

The significance of this lies in the fact that the very first step away from the saddle point is usually taken along this eigenvector. We show that along this eigenvector, $\mathbf{v}^{(1)}$ tends toward a finite limiting value at the saddle point that is incorrect. Thus, regardless of how small the step size is taken or with what numerical precision $\mathbf{v}^{(1)}$ is calculated, one will al-

ways get the wrong answer for $\mathbf{v}^{(1)}$ and for the RPH coupling parameters derived from it. Since the higher $\mathbf{v}^{(n)}$ depend on $\mathbf{v}^{(1)}$, they too will be in error. The correct values can only be obtained by stepping along the actual *curved* reaction path.

It is important to understand the distinction between the reaction path and the straight line path defined by the eigenvector. Although the two paths "meet" at the saddle point and (as we shall see) share the same path tangent $\mathbf{v}_0$ at the saddle point, only the reaction path is a solution to Eq. (2). The quantity $\mathbf{v}^{(1)}$ is the curvature of the solution to Eq. (2) which passes through any point of interest. If this point lies on the reaction path then $\mathbf{v}^{(1)}$ will be the curvature of the reaction path. If the point lies elsewhere, such as on the eigenvector, then $\mathbf{v}^{(1)}$ will not be the reaction path curvature. Each point in the sequence on the eigenvector path will correspond to a different solution to Eq. (2) whereas each point on the reaction path corresponds to the same solution to Eq. (2).

We define the eigenvector path as

$$\mathbf{x}(\alpha) = \alpha \mathbf{v}_0, \tag{C1}$$

where $\mathbf{v}_0$ is the reaction path tangent at the saddle point and α is the "arc length" or mass weighted distance from the saddle point.

In order to compute the curvature $\mathbf{v}^{(1)}$ at the point $\mathbf{x}(\alpha)$ we need the gradient and force constant matrix evaluated at this point. We obtain these by first expanding the energy in a Taylor series about the saddle point $\mathbf{x} = 0$:

$$E(\mathbf{x}) = \frac{1}{2}\mathbf{x}^\dagger \mathbf{F}_0 \mathbf{x} + \frac{1}{6}\sum_i \sum_j \sum_k G_{0_{ijk}} x_i x_j x_k + \cdots . \tag{C2}$$

The gradient and force constant matrix at an arbitrary point near the saddle point are then

$$g_i = \sum_j F_{0_{ij}} x_j + \frac{1}{2}\sum_j \sum_k G_{0_{ijk}} x_j x_k + \ldots \tag{C3}$$

and

$$F_{ij} = F_{0_{ij}} + \sum_k G_{0_{ijk}} x_k + \cdots . \tag{C4}$$

Substituting Eq. (C1) into Eqs. (C3) and (C4) gives

$$g_i(\alpha) = \alpha \left[\sum_j F_{0_{ij}} v_{0_j} + \frac{1}{2}\alpha \sum_j \sum_k G^0_{ijk} v_{0_j} v_{0_k} + \cdots \right] \tag{C5}$$

and

$$F_{ij}(\alpha) = F_{0_{ij}} + \alpha \sum_k G_{0_{ijk}} v_{0_k} + \cdots . \tag{C6}$$

In matrix form these can be written as

$$\mathbf{g}(\alpha) = \alpha(\mathbf{F}_0 \mathbf{v}_0 + \tfrac{1}{2}\alpha \mathbf{F}_0^{(1)} \mathbf{v}_0 + \cdots) \tag{C7}$$

and

$$\mathbf{F}(\alpha) = \mathbf{F}_0 + \alpha \mathbf{F}_0^{(1)} + \cdots , \tag{C8}$$

where $\mathbf{F}_0^{(1)}$ is the component of the third derivatives along the path tangent $\mathbf{v}_0$ [Eq. (13)] evaluated at the saddle point.

Substituting Eq. (C7) into Eq. (C5), the normalization constant at $\mathbf{x}(\alpha)$ becomes

$$c(\alpha) = \alpha\{\mathbf{v}_0^\dagger \mathbf{F}_0^2 \mathbf{v}_0 + \tfrac{1}{2}\alpha \mathbf{v}_0^\dagger (\mathbf{F}_0 \mathbf{F}_0^{(1)} + \mathbf{F}_0^{(1)} \mathbf{F}_0)\mathbf{v}_0 + \cdots\}^{1/2}, \tag{C9}$$

where we have retained terms only through the first power in α in the expression inside the brackets.

The path tangent evaluated at $\mathbf{x}(\alpha)$ is, by substituting Eqs. (C7) and (C9) into Eq. (2),

$$\mathbf{v}(\alpha) = \frac{[\mathbf{F}_0 \mathbf{v}_0 + (1/2)\alpha \mathbf{F}_0^{(1)} \mathbf{v}_0 + \cdots]}{[\mathbf{v}_0^\dagger \mathbf{F}_0^2 \mathbf{v}_0 + (1/2)\alpha \mathbf{v}_0^\dagger (\mathbf{F}_0 \mathbf{F}_0^{(1)} + \mathbf{F}_0^{(1)} \mathbf{F}_0)\mathbf{v}_0 + \cdots]^{1/2}} . \tag{C10}$$

Note that we have divided out the common factor α in the numerator and denominator. In the limit of small α, Eq. (C10) becomes $\mathbf{v}_0$. This can be seen by setting $\alpha = 0$ in the right-hand side of Eq. (C10) and using Eq. (14) to simplify the result. Thus as the saddle point is approached along $\mathbf{x}(\alpha)$ the path tangent approaches the correct value.

The value of the path curvature at $\mathbf{x}(\alpha)$ is obtained by substituting Eqs. (C8), (C9), and (C10) into Eq. (7). We will not reproduce this messy formula here. We note, however, that expanding the numerator of this result in powers of α gives the leading term as

$$\mathbf{F}_0^2 \mathbf{v}_0 - \frac{(\mathbf{v}_0^\dagger \mathbf{F}_0^3 \mathbf{v}_0)\mathbf{F}_0 \mathbf{v}_0}{(\mathbf{v}_0^\dagger \mathbf{F}_0^2 \mathbf{v}_0)}$$

which is zero by Eq. (14). This leaves a common factor α in the numerator and denominator which can be divided out as it was in Eq. (C10). Setting $\alpha = 0$ in the result then gives the limiting value of the curvature as

$$\lim_{\alpha \to 0} \mathbf{v}^{(1)}(\alpha) = [\mathbf{F}_0^{(1)} \mathbf{F}_0 - (\mathbf{v}_0^\dagger \mathbf{F}_0^{(1)} \mathbf{v}_0)\mathbf{F}_0 + \tfrac{1}{2}\mathbf{F}_0 \mathbf{F}_0^{(1)} - \tfrac{1}{2}(\mathbf{v}_0^\dagger \mathbf{F}_0^{(1)} \mathbf{v}_0)\mathbf{F}_0]\mathbf{v}_0/\mathbf{v}_0^\dagger \mathbf{F}_0^2 \mathbf{v}_0. \tag{C11}$$

This result is not the same as Eq. (19) although it also depends on third energy derivatives. It is therefore incorrect.

APPENDIX D: THE PROJECTION MATRIX

The projection matrix $\mathbf{P}$ can be defined as

$$\mathbf{P} = \mathbf{R} + \mathbf{v}\mathbf{v}^\dagger, \tag{D1}$$

where

$$\mathbf{R} = \sum_{i=1}^{6} \mathbf{v}_i \mathbf{v}_i^\dagger. \tag{D2}$$

Here the $\mathbf{v}_i$ are six orthonormal column vectors in the mass weighted Cartesian coordinates corresponding to overall translations and rotations and $\mathbf{v}$ is the unit tangent to the reaction path defined in Eq. (2). The $\mathbf{v}_i$ depend on geometry (and masses) alone and are therefore constructed indepen-

dently of energy considerations. Excluding the saddle point,[18] the path tanget $\mathbf{v}$ is proportional to the energy gradient and therefore has no component corresponding to translation and rotation in the absence of external forces.[1] We therefore focus on constructing $\mathbf{R}$, the contribution to $\mathbf{P}$ due to translations and rotations.

Our procedure will be as follows. We will first define six basis vectors which are not orthonormal but which span the translation–rotation subspace in Cartesian coordinates and have no components in the internal coordinate subspace. These will then be converted to mass weighted Cartesian coordinates and orthogonalized. $\mathbf{R}$ is then constructed from these orthogonalized vectors. The result [Eq. (D9) below] will involve only the basis vectors. The derivative of $\mathbf{R}$ will involve only the mass weighted basis vectors and their derivatives, which are readily obtained.

We choose as basis vectors the three translation displacements along each of the three Cartesian axes and the three infinitessimal displacements corresponding to rotations about these axes. Multiplying each of these vectors by the diagonal matrix of the square roots of the masses gives the basis vectors $\mathbf{b}_i$ in the mass weighted coordinates

$$
\mathbf{b}_1 = \begin{pmatrix} \sqrt{m_1} \\ 0 \\ 0 \\ \vdots \\ \sqrt{m_N} \\ 0 \\ 0 \end{pmatrix}, \quad
\mathbf{b}_2 = \begin{pmatrix} 0 \\ \sqrt{m_1} \\ 0 \\ \vdots \\ 0 \\ \sqrt{m_N} \\ 0 \end{pmatrix}, \quad
\mathbf{b}_3 = \begin{pmatrix} 0 \\ 0 \\ \sqrt{m_1} \\ \vdots \\ 0 \\ 0 \\ \sqrt{m_N} \end{pmatrix},
$$

$$
\mathbf{b}_4 = \begin{pmatrix} 0 \\ \sqrt{m_1}z_1 \\ -\sqrt{m_1}y_1 \\ \vdots \\ 0 \\ \sqrt{m_N}z_N \\ -\sqrt{m_N}y_N \end{pmatrix} = \begin{pmatrix} 0 \\ Z_1 \\ -Y_1 \\ \vdots \\ 0 \\ Z_N \\ -Y_N \end{pmatrix},
$$

$$
\mathbf{b}_5 = \begin{pmatrix} -\sqrt{m_1}z_1 \\ 0 \\ \sqrt{m_1}x_1 \\ \vdots \\ -\sqrt{m_N}z_N \\ 0 \\ \sqrt{m_N}x_N \end{pmatrix} = \begin{pmatrix} -Z_1 \\ 0 \\ X_1 \\ \vdots \\ -Z_N \\ 0 \\ X_N \end{pmatrix}, \tag{D3}
$$

$$
\mathbf{b}_6 = \begin{pmatrix} \sqrt{m_1}y_1 \\ -\sqrt{m_1}x_1 \\ 0 \\ \vdots \\ \sqrt{m_N}y_N \\ -\sqrt{m_N}x_N \\ 0 \end{pmatrix} = \begin{pmatrix} Y_1 \\ -X_1 \\ 0 \\ \vdots \\ Y_N \\ -X_N \\ 0 \end{pmatrix},
$$

where x_i, y_i, and z_i are the Cartesian coordinates of atom i and X_i, and Y_i, and Z_i are the mass weighted Cartesian coordinates. We let $\mathbf{W}$ be any 6×6 transformation matrix which produces orthonormal $\mathbf{v}_i$'s from the basis vectors $\mathbf{b}_i$:

$$
\mathbf{v} = \mathbf{b}\mathbf{W}, \tag{D4}
$$

where $\mathbf{v}$ is the $3N \times 6$ matrix whose columns are the $\mathbf{v}_i$ and $\mathbf{b}$ is the corresponding matrix of basis vectors. The matrix $\mathbf{R}$ then becomes

$$
\mathbf{R} = \mathbf{v}\mathbf{v}^\dagger = \mathbf{b}\mathbf{W}\mathbf{W}^\dagger\mathbf{b}^\dagger. \tag{D5}
$$

Since any real matrix $\mathbf{W}$ can be written as the product of a symmetric matrix and an orthogonal matrix, Eq. (D5) shows that only the symmetric part of $\mathbf{W}$ contributes to $\mathbf{R}$. Therefore, without loss of generality $\mathbf{W}$ can be regarded as symmetric. From the orthonormality condition we have

$$
\mathbf{v}^\dagger\mathbf{v} = \mathbf{W}^\dagger\mathbf{b}^\dagger\mathbf{b}\mathbf{W} = \mathbf{I}, \tag{D6}
$$

or, taking $\mathbf{W}$ to be symmetric ($\mathbf{W} = \mathbf{W}^\dagger$):

$$
\mathbf{W}^2 = \mathbf{W}\mathbf{W}^\dagger = \mathbf{S}^{-1}, \tag{D7}
$$

where $\mathbf{S}$ is the 6×6 "overlap" matrix

$$
\mathbf{S} = \mathbf{b}^\dagger\mathbf{b}. \tag{D8}
$$

$\mathbf{R}$ thus becomes

$$
\mathbf{R} = \mathbf{b}\mathbf{S}^{-1}\mathbf{b}^\dagger. \tag{D9}
$$

Using the definitions of the $\mathbf{b}_i$ [Eq. (D3)] $\mathbf{S}$ can be written as

$$
\mathbf{S} = \begin{pmatrix}
M & 0 & 0 & 0 & -\Sigma m_i z_i & \Sigma m_i y_i \\
 & M & 0 & \Sigma m_i z_i & 0 & -\Sigma m_i x_i \\
 & & M & -\Sigma m_i y_i & \Sigma m_i x_i & 0 \\
 & & & \Sigma m_i(y_i^2 + z_i^2) & -\Sigma m_i x_i y_i & -\Sigma m_i x_i z_i \\
 & & & & \Sigma m_i(x_i^2 + z_i^2) & -\Sigma m_i y_i z_i \\
 & & & & & \Sigma m_i(x_i^2 + y_i^2)
\end{pmatrix} \tag{D10}
$$

in the nonmass weighted Cartesian coordinates. M is the total mass. We note from Eq. (D10) that the overlap of a translational basis vector and a rotational vector is proportional to a component of the center of mass position, e.g.,[19]

$$
\mathbf{b}_1^\dagger\mathbf{b}_5 = -\sum_i m_i z_i = -M z_{\text{c.m.}}, \tag{D11}
$$

and that the rotation–rotation overlaps give elements of the moment of inertia tensor in center of mass coordinates. The

matrix S is therefore diagonal if one chooses the coordinate origin to be the center of mass and the x, y, and z axes to lie along the principal inertial axes. This, however, is not necessary.[20]

The derivative of $\mathbf{R}$ with respect to motion along the path tangent is, by differentiating Eq. (D9) and using Eq. (D8):

$$\frac{d\mathbf{R}}{ds} = \mathbf{Q} + \mathbf{Q}^{\dagger}, \tag{D12}$$

where

$$\mathbf{Q} = (\mathbf{I} - \mathbf{R}) \frac{d\mathbf{b}}{ds} \mathbf{S}^{-1} \mathbf{b}^{\dagger}. \tag{D13}$$

The derivative $d\mathbf{b}/ds$ is easily constructed. The first three columns are zero and the last three involve only the derivatives of the mass weighted Cartesian coordinates with respect to s. These are just elements of the path tangent $\mathbf{v}$ [Eq. (2)]. In other words if the mass weighted coordinates in $\mathbf{b}_4$, $\mathbf{b}_5$, and $\mathbf{b}_6$ are replaced with the corresponding elements of $\mathbf{v}$, the result is $(d\mathbf{b}_4/ds)$, $(d\mathbf{b}_5/ds)$, and $(d\mathbf{b}_6/ds)$.

Using Eqs. (D1), (D2), and (D9) we have for the derivative of the projection matrix

$$\frac{d\mathbf{P}}{ds} = \mathbf{Q} + \mathbf{Q}^{\dagger} + \mathbf{v} \frac{d\mathbf{v}^{\dagger}}{ds} + \frac{d\mathbf{v}}{ds} \mathbf{v}^{\dagger}, \tag{D14}$$

where $(d\mathbf{v}/ds)$ is the path curvature vector given by Eq. (7). At nonstationary points Eq. (D14) involves at most second energy derivatives and is therefore computed exactly in the LQA. At stationary points Eq. (D14) is not needed.

[1] W. Miller, N. Handy, and J. Adams, J. Chem. Phys. **72**, 99 (1980).

[2] W. Miller, in *The Theory of Chemical Reaction Dynamics*, edited by D. C. Clary (Reidel, Dordrecht, 1986), p. 27.

[3] D. Truhlar and B. Garrett, Annu. Rev. Phys. Chem. **35**, 159 (1986).

[4] D. Truhlar, R. Steckler, and M. Gordon, Chem. Rev. **87**, 217 (1987).

[5] D. Truhler, F. Brown, R. Steckler, and A. Isaacson, in *The Theory of Chemical Reaction Dynamics*, edited by D. C. Clary (Reidel, Dordrecht, 1986), p. 285.

[6] (a) C. Doubleday, R. Camp, H. King, J. McIver, D. Mullally, and M. Page, J. Am. Chem. Soc. **106**, 447 (1984); (b) C. Doubleday, J. McIver, M. Page, and T. Zielinski, *ibid.* **107**, 5800 (1985); (c) C. Doubleday, M. Page, and J. McIver, J. Mol. Struct. (in press); (d) C. Doubleday, J. McIver, and M. Page, J. Phys. Chem. (submitted).

[7] D. Truhlar, A. Isaacson, and B. Garrett, in *Theory of Chemical Reaction Dynamics*, edited by M. Baer (Chemical Rubber, Boca Rotan, 1985), Vol. IV, p. 65.

[8] (a) K. Ishida, K. Morokuma, and A. Komornicki, J. Chem. Phys. **66**, 2153 (1977); (b) K. Muller and L. Brown, Theor. Chim. Acta **53**, 75 (1979); (c) M. Schmidt, M. Gordon, and M. Dupuis, J. Am. Chem. Soc. **107**, 2585 (1985); (d) H. Schlegel, Adv. Chem. Phys. **67**, 249 (1987).

[9] K. Fukui, Acc. Chem. Res. **14**, 363 (1981).

[10] See, for example, *Geometrical Derivatives of Energy Surfaces and Molecular Properties*, edited by P. Jorgensen and J. Simons (Reidel, Dordrecht, 1986).

[11] P. Pechukas, J. Chem. Phys. **64**, 1516 (1976).

[12] This follows by induction. $\mathbf{T}_1$ is proportional to third derivatives. Therefore, so is $\mathbf{v}_0^{(1)}$ by Eq. (17). $\mathbf{T}_2$ is proportional to $\mathbf{v}_0^{(1)}$ and third and higher derivatives. Therefore, so is $\mathbf{v}_0^{(2)}$ by Eq. (17), etc.

[13] These devices (Ref. 8) appear to work quite well. One should note, however, the following formal objection to their use. Of all the solutions to Eq. (2) only one terminates at the saddle point. This is the reaction path. It cannot be defined or calculated without referencing the saddle point. When one has left the path one attempts to return to it using only locally available information in which reference to the saddle point has been lost. Therefore, one cannot always expect these devices to work. The problem of determining the path from local information only is discussed in Ref. 14.

[14] D. Hoffman, R. S. Nord, and K. Ruedenberg, Theor. Chim. Acta **69**, 265 (1986).

[15] R. Camp and H. King, J. Chem. Phys. **77**, 356 (1982).

[16] Given third derivative information, one can devise various alternative methods of approximating the reaction path, none of which we have yet investigated. In generalized normal coordinates, for example, the Taylor series including the second and diagonal third derivatives can be summed exactly and the remaining third derivatives included by partial summing to high order.

[17] This, however, will never occur in practice for many-dimensional problems, since it requires that somewhere between the saddle point and products the path tangent must simultaneously satisfy Eq. (2) and the gradient extremal condition (that the path tangent is an eigenvector of F) (Ref. 14). While a gradient extremal path might cross the reaction path in a two-dimensional problem it is improbable in many dimensions.

[18] At the saddle point, the rotations, translations, and path tangent are already eigenvectors of F, so that projecting them out is unnecessary. Although K and F share a set of eigenvectors at the saddle point, they are not identical. The negative eigenvalue of F corresponding to the path tangent becomes a zero eigenvalue of K.

[19] This reflects the fact that unless the center of mass is at the origin, a rotation about the origin contains a translational component.

[20] If desired, vectors $\mathbf{v}_i$ which correspond to translations along and rotations about the principle inertial axes can be obtained from the 6×6 column eigenvector matrix U and the diagonal matrix of eigenvalues $\boldsymbol{\epsilon}$ of S. The result is $\mathbf{v} = \mathbf{b} \mathbf{U} \boldsymbol{\epsilon}^{-1/2}$.